Chapter 10
Real-Time Programmable Closed-Loop Stimulation/Recording Platforms for Deep Brain Study

Hung-Chih Chiu and Hsi-Pin Ma

Abstract Biomedical systems have expanded markedly in recent years, spreading into many areas of human life. Rapid advances in biological science have led to the creation of novel electrical circuits and signal processing methods and the development of tools for diagnosing and treating human diseases. Many biomedical engineering researchers have developed novel tools designed to tackle specific medical conditions.

The instruments used represent an interface between biology and electronics. These interfaces enable biological phenomena to be quantified and characterized, thus allowing the biological processes underlying them to be elucidated. A typical interface comprises a sensor or electrode for detecting some biological parameter, the signals from which are then amplified and converted into a digital form. These digital data can be processed by hardware or transferred to a personal computer for closed-loop control, long-term storage, and more precise signal processing. The guidelines for such signal processing algorithms require low complexity, short latency, high sensitivity, and accurate characterization. Microprocessors are used to make the design of an electronic algorithm flexible and adaptable. Depending on the requirements of a specific application, the data can be transferred through wired or wireless links. Communication can be achieved using widely available and clearly defined technical specifications.

This chapter discusses the main hardware and software components used in closed-loop deep brain stimulation systems and describes the evaluation procedures that are used to ensure that the system performs as specified. Even when the system parameters can change with the physiological characteristics, a closed-loop control system can accurately extract the signals of interest.

Keywords Neural recording/stimulation • Closed-loop stimulation platform • Deep brain stimulation • Parkinson's disease • Time-frequency signal processing • Phase analysis • Phase synchrony • EEG • Local field potential

H.-C. Chiu • H.-P. Ma (✉)
Department of Electrical Engineering, National Tsing Hua University, Hsinchu, Taiwan
e-mail: hp@ee.nthu.edu.tw

C.-M. Kyung et al. (eds.), *Smart Sensors and Systems*,
DOI 10.1007/978-3-319-33201-7_10

10.1 Introduction

Bioelectronic systems are used to measure and quantify physiological parameters within the human body and to treat certain medical conditions. The interface with the human body makes it possible to investigate the biological world and the function of human body systems. Compared with conventional biomedical electronic systems based on digital signal processing (DSP) units, a real-time electronic system can provide a programmable approach to recording and stimulating the system, low-complexity DSP, and a closed-loop strategy for recording feedback from the stimulated nuclei.

Electrical stimulation systems have been used to study the behavior of neurons in the brain [1–4]. Various therapies use deep brain stimulation (DBS) to alleviate neurological disorders and to treat Parkinson's disease [5], tremors [6], epilepsy [7, 8], depression [9], cluster headaches [10, 11], and other maladies [12, 13]. In order for DBS therapy to be effective, the electrical pulses used must be of high frequency. Many previous studies have quantified the energy used in neural activities. This has been done by calculating the power density in a particular bandwidth of the brain, because neural synchrony exhibits large variability in amplitudes and recurrence. There is increasing evidence to suggest that deep electrical stimulation of brain structures suppresses neuronal synchrony at the basal ganglia (BG) [14]. Suppression of neuronal synchrony in Parkinson's disease usually involves open-loop deep electrical stimulation of brain structures using local field potentials (LFPs) [15]. Open-loop deep electrical stimulation delivers preprogrammed electric signal patterns, but an effective feedback loop for maintaining the neurotransmitters cannot be selected. By contrast, a closed-loop stimulation strategy has a considerably stronger effect while preserving battery life and allowing precise control of the functional electrical stimulation of the brain. However, closed-loop stimulation strategies are not yet well enough understood to allow the selection of the stimulation conditions. Few guidelines are available covering the selection of appropriate closed-loop stimulation strategies, in which the signal characteristic changes in the power spectra of the LFPs [16], or the phase is synchronous in the specific frequency band [17]. Closed-loop stimulation strategies must take account of power consumption and battery life. A long-term objective is to develop a system that can automatically adjust the stimulation strategies to achieve suppression of neuronal synchrony based on the electrical signals from the deep brain. Closed-loop stimulation platforms for deep brain study are discussed in detail in this chapter, which is organized as follows.

The remainder of this chapter is organized as follows: design considerations for closed-loop stimulation strategies are discussed in Sect. 10.2. Standard closed-loop DBS and recording system design are described in Sect. 10.3. Section 10.4 discusses closed-loop control policies and DSP. Section 10.5 presents an integrated electronic and signal processing system, including system architecture, firmware design, mathematical instruments for measuring neural activity, and closed-loop neural phase synchrony detection. Section 10.6 offers some conclusions.

10.2 Considerations for Closed-Loop System Design

In closed-loop DBS, bioelectrical signals are used to extract information from a biological system. These signals exhibit different electrical characteristics, including different levels of complexity, because an organ comprises multiple tissue types and functional units, but is composed of cells that have common features. The electrical signal received will reflect these similar cell features, but intracellular variation will have an effect on the electrical properties. The electrical properties can be captured by devices as simple as a closed-loop device on the skin surface or microelectrodes placed in direct contact with the biological tissue. The characteristics of the bioelectrical signals place further constraints on the design and application of biomedical instrumentation systems. Novel closed-loop design strategies must be considered for the instrumentation systems used in medical facilities and research centers. In the design of a biomedical system, the following factors must be considered:

(1) *Energy source*: The human or animal body can provide an original source for the DBS system. Many biomedical systems allow human health to be monitored by an implanted device. Different body parts produce different signals. Bioelectric signals are produced by muscles and neuron cells, with the cell potential providing the electricity source.

(2) *Sensors*: A sensor is used to convert the physical condition or property into an electrical signal with specific characteristics. Factors including noise and electrode impedance can influence the choice of analog front-end architecture. For example, the electrode impedance is not dependent on the electrical properties of the materials, but on chemical reactions at the interface between the electrode and the electrolyte [18]. In general, commercial electrodes for bioelectrical recording have an impedance of 1 kHz, a range from 10 to 1000 kΩ, and capacitance values of between 100 and 350 pF. Hence, the amplifier must be properly designed to accommodate such large capacitive impedance. In real applications, the electrode impedance includes thermal noise [19], whose background fluctuations generate 5–10 μV over 10 kHz.

(3) *Signal acquisition and processing systems*: Converting the physical condition into an electrical signal can assist the user of the closed-loop DBS system. Signal acquisition mainly involves the use of function blocks such as amplifiers, A/D converters, D/A converters, wireless circuits, and digital control circuits.

After the biosignals have been converted into a digital form, the data must be passed through a closed-loop processing algorithm. Digital recording must be tightly controlled as it affects both the signal traces produced and the performance of the algorithm. Effective control of these parameters sets the system state under which the processing algorithm is characterized to the expected condition. For example, different kinds of bioelectrical sensing systems require different sampling rates, electrodes, and closed-loop control policies. All of them must be designed to a specification. In real clinical applications, motion artifacts from the patient may be

produced while recording the electrical signal, and such artifacts can significantly affect algorithm performance.

(4) *System Latency*: The operation of closed-loop system control can be divided into three steps: data acquisition, processing, and event detection [16]. Each step can be controlled by a digital core or by independent programs that communicate with each other via defined protocols. Each step introduces time and delay latency. If this latency is too long or unpredictable, it may interfere with the real-time closed-loop stimulation.

The time period for data acquisition in a sample block is controlled by the system protocol. The exact latency depends on the type of A/D converter used. As the data stored in the buffers is processed by the algorithms, the processing latency depends on the complexity of processing and the clock speed. The detection latency is determined by a number of factors that successively trigger the stimulator. Therefore, assessment of the timing characteristics is a critical issue in the development of closed-loop systems. Exact latency can be achieved with careful implementation.

(5) *Monitor system*: The monitor system is the bridge between the biomedical system and the host PC. Results can be displayed on a user-friendly graphical user interface. The monitor system can be numerical or graphical, or show features characteristic of the biomedical activity being investigated.

10.3 General Closed-Loop Deep Brain Stimulation and Recording System Design

The efficacy of DBS in treating neurological disorders such as movement disorders, pain, epilepsy, and psychiatric disorders has been demonstrated, and a closed-loop control policy can further improve these treatments by precisely monitoring the neurotransmitters. A typical closed-loop DBS system can be characterized as follows: (1) an adaptive DBS system can be used to measure and analyze a chosen variable reflecting ongoing pathological changes in the patient's clinical condition to derive new stimulation settings [20]. (2) Key elements that can be added to the generalized bi-directional brain-machine interface to facilitate research on chronic conditions include multichannel LFP amplification, accelerometers, spectral analysis, and wireless telemetry for data uploads [21]. (3) Closed-loop DBS systems have further developments in the charge transfer mechanisms at the electrode and tissue interface. This can be used to investigate the symptoms of neurological disorders and any side effects that may occur. Transgenic animals may be used in the testing of systems that improve the energy efficiency of the stimulation [22, 23]. (4) Closed-loop stimulation methods can dissociate changes in BG discharge rates and patterns, providing insights into the pathophysiology of PD [16]. This will have a significantly greater effect on akinesia. (5) While modulating neural activity is an effective treatment for neurological diseases, systems have been demonstrated that can identify a biomarker and the transfer functions of

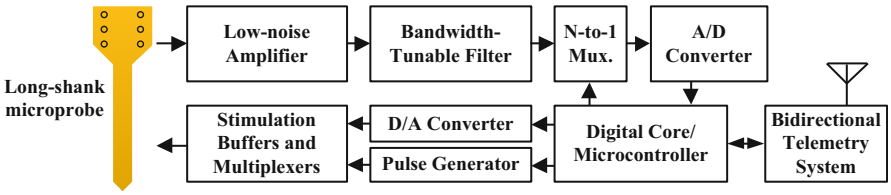

Fig. 10.1 System architecture of a real-time programmable closed-loop stimulation and recording platform comprising a neural recording system, a stimulation system, and a digital core

different stimulation amplitudes in a chronic animal mode [24]. (6) Signal unit recording can be done using a variety of brainwave recording techniques, and these parameters can be used for closed-loop activation of spinal circuitry below the level of injury [25]. A typical model of a closed-loop DBS system is illustrated in Fig. 10.1.

The DBS system mainly comprises a monitor and signal acquisition system, a microprocessor, a stimulator, and peripheral interconnection components. All the subsystems must be properly calibrated. Microprocessors form the kernel of the DBS, and their incorporation into biomedical systems has added computing power and greater control capability. The signal processor is used to acquire data, control the transducer, and provide closed-loop DSP. The performance of the signal processing algorithm is assessed prior to hardware implementation, and an input biosignal is passed through the algorithm. It must be demonstrated through simulation that the signal processing algorithm is rigorous, accurate, and produces reproducible data [23, 26]. The wider availability of microcontrollers has provided functional sub-circuits that offer both manual programming and automatic digital control, which can help reduce the complexity of the circuit interface. Compared with conventional biomedical electronic systems using DSP, the real-time closed-loop electronic system offers programmable recording and stimulation, a low-complexity and short latency DSP, and a closed-loop strategy for measuring feedback within the stimulated nuclei. In biomedical applications where low-power operation is a major concern, energy efficiency when performing a specific task becomes a significant consideration. These issues are discussed in Sect. 10.3.1.

10.3.1 Neural Recording System

The deep brain signals measured by the sensors are amplified to levels suitable for signal processing. The electrical signals are on the order of microvolts to millivolts, for example, 10–300 μV for LFPs, 1 μV for evoked potentials, and 10–20 μV for EEGs [27]. Two different methods are used for brainwave recording. One is called monopolar recording, in which a channel potential is compared to a reference electrode placed at a distant location. Monopolar recording involves amplitudes up to 50 μV, which are more sensitive to global neural activity and motion artifacts.

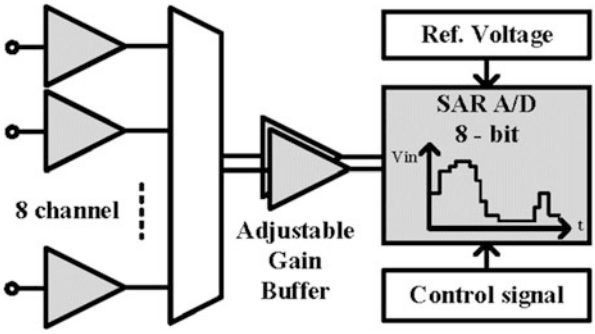

Fig. 10.2 The architecture of the recording system

The other method is called bipolar recording, in which a channel is compared to any one of the other channels, at amplitudes of approximately 5–20 μV, depending on the electrode distance and location. This method is less sensitive to noise and motion artifacts and more sensitive to localized neural activity.

As already noted, in a DBS application, the neural activities are captured by the probes or electrodes, and the bioelectrical signals generated can be fed into a microprocessor. Generally, amplifiers must be used without distortion and suppress system or environmental noise. Figure 10.2 shows a schematic of a recording system, which comprises a low noise amplifier and successive approximation (SAR) A/D conversion. The amplifier has an analog output or is integrated with the SAR A/D unit.

10.3.1.1 Amplifier

In principle, biosignal amplifiers are differential amplifiers which can measure a potential difference and contain high-impedance input circuits with a high common mode rejection ratio (CMRR) of between 60 and 110 dB. High CMRR can minimize noise from the power line and AC inductive power link. Ideally, the amplifier can amplify the difference between the brain signals from two input electrodes and eliminate the signal components that are common to both signals. When electronics are applied to the electrodes before the preamplifier or filtering, the CMRR of the amplifier may be reduced. For example, neural spikes contain high-frequency information (e.g., 300–6 kHz) and have a high-pass cutoff of around 6 kHz [28]. Analog filtering allows these high-frequency signals to pass through unattenuated. The anti-aliasing filter includes a low-pass cutoff, and the sampling rates must be high enough to sense high-frequency signals.

Amplifiers designed for deep brain signal recording must meet specific requirements. First, a high sampling rate over 20 kHz is required by the A/D converter, so an anti-aliasing filter must be incorporated. These filters typically remove high-frequency signals (e.g., higher than 500 Hz), in order to retain the LFPs waveform. Second, the input impedances must be higher than the probe impedance.

A typical neural probe impedance is in the range of 1–1000 kΩ at 1 kHz. The input impedance should be at least 100 times larger than that of the probe. Pre-amplifiers with high impedance are therefore commonly used at the buffering stage in the differential amplifier [29, 30].

10.3.1.2 A/D Converter

Many modern biomedical recording systems provide multichannels with high sampling rates, but the amplitude resolution and dynamic range of the A/D converter has a significant effect on the frequency range of the electrical signals recorded. In a deep brain recording system, an SAR A/D is commonly used to test the accuracy of the substrate resistance network, because it is widely applied to bio-chips and complete analysis methods of the SAR A/D. The advantages of this architecture are a low latency-time, high accuracy, and low-power consumption, with maximum sample rates of 2–5 MHz.

After neural signals are amplified, the digitized signal from each amplifier cycles many times per second, and this is called the sampling rate. The sampling frequency must satisfy the Nyquist criterion and must be at least 2 times larger than the highest frequency occurring in the biosignal. If the system does not satisfy the Nyquist criterion, the information contained in the sequence of samples will be distorted by aliasing [31]. In practice, the sampling rate may be several times higher than the recording bandwidth, since an anti-aliasing filter cannot filter out the higher frequency signals.

As described above, the brain signal is recorded using a multichannel differential amplifier. The signal input from different amplifiers and the entire analog signal must be digitized simultaneously. However, the digitization system contains a single A/D converter and the samples are acquired at different times. Several methods are available to address this problem: (1) a sample-and-hold method can hold the analog signal until the digitizer is ready to read the data or (2) a high sampling rate can reduce the sample time between each channel. A more detailed discussion of sampling and digitizing theory can be found in this reference [32].

10.3.2 Neural Stimulation System

The stimulation system consists of a responsive stimulator, electrode leads, and a function of the programmable parameters [33]. The stimulator is capable of communication with external components such as baseband circuits, a microcontroller, or wireless telemetry. The operator can use the bi-directional telemetry system to rewrite the digital core firmware and adjust the stimulator setting. The sensing data transmitter communicates with the central data management system where data can be stored and reviewed by physicians.

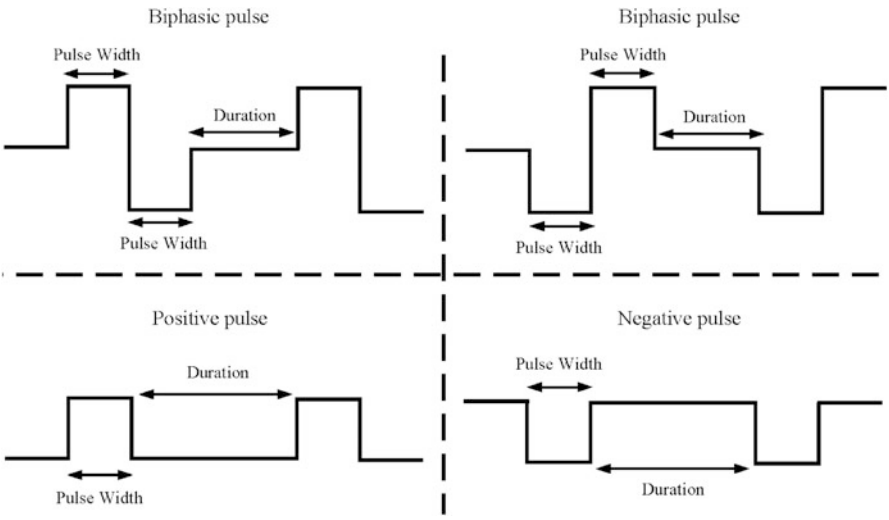

Fig. 10.3 Types of stimulation pulse shape, width, and duration

In principle, the closed-loop stimulator is a multi-functional stimulation device, which performs the following functions: (1) responsive stimulation, (2) digital to analog (D/A) decoding, and (3) battery voltage monitoring. Closed-loop responsive stimulation is controlled by a detection system in the digital core. As shown in Fig. 10.3, a range of stimulation parameters can be adjusted, including the stimulus voltage, stimulation frequency, and the pulse width and duration [34]. As discussed above, stimulation can be monopolar or bipolar. Monopolar stimulation requires the same polarity, while in bipolar stimulation the input is cathodic and the reference potential is anodic.

The D/A decoder is used to classify the digital patterns. The stimulation parameters can identify the pattern across the electrographic events and detection algorithm. After the stimulation parameter is set, the stimulator transmits the stimulation current to the tissue via the neural probe. A closed-loop stimulation control system can automatically evaluate the neural disorder and suppress neuronal synchrony. In addition, closed-loop stimulation incorporating battery voltage monitoring offers significantly extended battery life and reduced power consumption.

10.3.3 Digital Integrated Circuits

The digital circuit is the core of the closed-loop DBS system, performing data acquisition, DSP, sensor interfacing, and event detection. The generic architecture of the digital module is presented in Fig. 10.4.

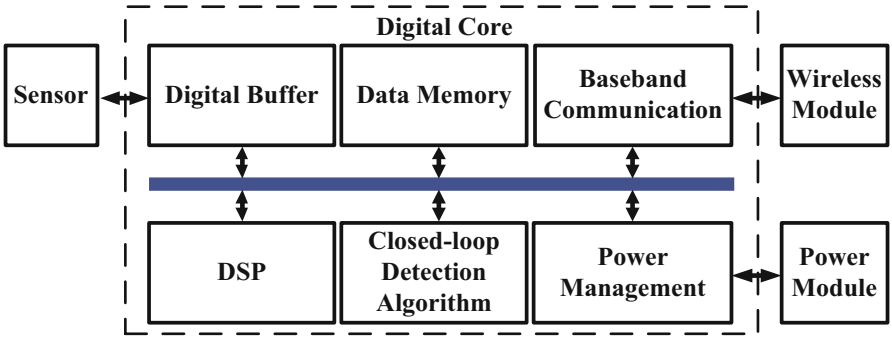

Fig. 10.4 A general architecture of digital core in closed-loop system

The DSP component of a closed-loop system performs two essential functions: feature extraction and control policy. Feature extraction is used to identify signal characteristics from the raw data and to convert the data into the mathematical domain. Data can be transferred to the frequency domain using Fourier transform or by assessment of power spectra, coherence, or cross-correlation coefficients [35, 36]. In closed-loop system design, it is essential that the signal processing is dynamic to allow optimal control policies to be applied to the digital circuits. Detection methods have therefore been adapted to fit the low-complexity constraints on the DSP. It is also important to take account of the system control policy when considering the closed-loop function for different depths of the brain. These functions include turning the stimulator on and off, feedback control of specific features, evaluation of the detection latency, and switching between the various subsystem interfaces.

The digital buffer is the bridge between the analog front-end and the digital circuits and can be used to acquire the digital signals from the subject. Different kinds of bioelectrical signal require different sampling rates. However, when the buffer cannot be merged with the digital module, tunable bus encoder technology can be used to reduce the biosignal activity [37].The digital buffer requires clocks, because different levels and functions of the system require different clock frequencies in the digital domain. As each subsystem can decrease the frequency range for different algorithms or baseband circuits, system power consumption and battery life can be substantially affected. For example, a sleep mode can be used to reduce the system power consumption. This mode is controlled by a low clock manager, and the controller can shut off the system main clock. Synchronous circuit design is very critical in a system which includes two different clock domains. Hence, the design of a state machine is a critical issue.

10.4 Closed-Loop Control Policy and Digital Signal Processing

Biomedical signals carry information on a biological system. Biomedical measurement systems must be secure and perform as intended to allow medical personnel to make precise diagnoses and choose the correct treatments. To satisfy these requirements, the digital core must meet numerous standards and regulations for each biomedical signal processing method used in the system. However, precise detection of the target signal and noise components remains a critical issue.

Most closed-loop stimulation systems use components of brain signals that are clearly characterized as biosignal features. They are detected using data processing algorithms that continuously monitor the brain activity. A data processing algorithm analyzes each incoming sample block from each biosignal to identify these features. The detection system is capable of comparison and specific detection. In general, two detection methods, linear and nonlinear, are used by the detection algorithm. These processing methods can be applied independently or to integrated circuits, and electrical stimulation systems can also be configured for detection. After the signal is processed, feedback is required to improve the detection of the probes at different depths in the brain. As the signals may include ECoG from the cortex or from the subthalamic nucleus in the deep brain, they clearly supply different amounts of information, based on the frequency domain [38]. The detection system must be able to adapt its parameters to improve the accuracy of the closed-loop stimulation system. Possible improvements in signal processing fall into the following categories: (1) extraction of information in more useful forms, (2) predictive data to anticipate the information from a specific signal, (3) data compression, and (4) filtering out of nonessential information, such as power-line noise or motion artifacts. Thus, it is common for a DBS system to incorporate features such as digital filters, linear and nonlinear combinations, or other modifications.

10.4.1 Digital Filtering

Digital filters are central to all signal processing systems. Each sample of the digitized signal is passed through a specific type of filter. Digital filters are used to filter out unwanted noise or artifacts from the biosignal to enhance the quality of the signal and prepare it for closed-loop detection.

If input data x[n] enter the filter sequentially, the output data y[n] is the weighted sum of the current and past values, and is given by:

$$y[n] = \sum_{i=0}^{M} a_i x[n-i] - \sum_{i=1}^{N} b_i y[n-i],$$

where x[n−i] is the past input data, y[n−i] is the past output data, the a_i and b_i parameters are the weights, and M and N are the numerical data lengths. The filtered output data have the same number of samples, in which the first sample of y[n] corresponds to the first sample of x[n]. Filters that depend on current and past data are known as causal filters. In real-time applications, causal filtering is necessary because future input and output data are not yet available. A simple example is the computation of a moving average. When computing a moving average, the signal passes through the filter, and the filter data is equal to the sum of the past input samples (N) each weighted by 1/N. This filter attenuates the high frequencies and preserves the low frequencies. The guidelines for developing closed-loop control demand low complexity and short latency. The sums of the past N consecutive samples have to be considered in the optimal range.

10.4.2 Time Domain Signal Processing Techniques

Linear signal processing can incorporate a number of different procedures. These can be categorized as (1) block processing, (2) peak detection and integration, and (3) wave detection. In a closed-loop system, it is desirable for the signal processing to occur in real time. Before being fed into the processing algorithm, the incoming raw data samples are segmented consecutively, either with or without overlapping. If the signal features are computed more frequently than is necessary, the system will consume additional computational time and power. In efficient real-time implementations, therefore, the data window size and overlap of the blocks should closely reflect the processing algorithm, detection latency, and available processing power.

Peak detection and integration are the most straightforward and simple methods for achieving this. Peak detection determines the maximum or minimum value of the data in a window and uses this value as the feature. Features can be averaged or integrated to provide more detailed information on the time domain. These methods can also be applied to the detection of transient spectrum peaks in the frequency domain.

Wave detection is calculated as the sum of the amplitude changes within a time window. This method is mainly used to measure the complexity of the fractal dimensions of a deep brain signal. The wave difference or the ratio of the average change between a short and long window can be used to determine whether the signal complexity is increasing or decreasing.

10.4.3 Frequency Domain Signal Processing Techniques

Deep brain signals have continuous amplitude and frequency modulated oscillations. A number of researchers are tracking these changes in the frequency domain. Much of frequency domain theory is based on Fourier analysis, which transforms time domain data into a frequency domain representation. Depending on the specific constraints or objectives, techniques such as fast Fourier transform (FFT) or autoregressive (AR) modeling are used. An FFT spectrum tracks the brain signal at a corresponding frequency, and the power spectrum of the FFT can be obtained by squaring the magnitude. This is an efficient implementation method for brain signals in a closed-loop system. AR modeling can use higher spectral resolution for signal window sizes shorter than those used in FFT. The development of small window sizes is necessary for closed-loop systems, because long latencies significantly affect real-time operations.

10.5 A Design Case: A Real-Time Closed-Loop Neurostimulation System Based on Neural Phase Synchrony Detection

10.5.1 Introduction to Closed-Loop Neurostimulation System

Parkinson's disease (PD) is one of the most prevalent diseases in people aged 50–60 years [39]. The introduction of levodopa (L-dopa) in the late 1960s caused a sharp decline in the surgical treatment of PD. Oral administration of L-dopa, which transforms into dopamine in the basal ganglia (BG), is a widely adapted chemical therapy for PD [40, 41]. However, long-term use of L-dopa is associated with motor fluctuations and dyskinesia [42], and DBS of BG nuclei is increasingly considered a highly effective and adjunctive therapy for PD symptoms [43–45], such as tremor and dystonia; moreover, it limits drug-induced side effects.

Numerous studies have quantified the energy in neural activities, which is measured by calculating the power density in a particular bandwidth of the brain because neural synchrony exhibits large amplitude and recurrence variability. Furthermore, increasing evidence indicates that deep electrical stimulation of brain structures suppresses neuronal synchrony at both BG [14]. Suppressed neuronal synchrony in PD usually involves open-loop deep electrical stimulation of brain structures such as LFPs [46]. Open-loop deep electrical stimulation delivers preprogrammed electric signal patterns, but the effective feedback loop for maintaining neurotransmitters cannot be chosen. By contrast, closed-loop stimulation strategy has a considerably stronger effect with preserving battery life, decreased neural synchronization, and an ideal control policy for feedback within the stimulated nuclei. For instance, neurological disorders are ameliorated when stimulation is based on electrical signal feedback and matched to the

frequency of the abnormal synchronization [16]. In addition, characteristic changes in the power spectra of LFPs have been identified after DBS of the BG, and an adaptive model based on recursive identification by the brain has been developed [17]. However, the power spectra do not consider the dynamic phase synchronous properties exhibited by the additional information in closed-loop strategies. The phase synchronous in the specific frequency band is a marker of neurological disorders in PD such as the beta band synchronization of BG is associated with the motor symptoms, such as the hypokinetic symptoms [47] and associated symptoms were reduced by different therapies [48]. Hence, the phase synchronous of neurophysiologic signals is used to estimate the neurological disorders at beta frequency oscillations. With this framework, this study is to develop a programmable closed-loop stimulation control system that automatically evaluates the neural phase synchrony to achieve reduction of motor symptoms.

Synchronous neural detection hardware that precisely controls intracortical microstimulation [49], closed-loop spike detection algorithms for triggering electrical stimulation, [50], and electroencephalograph (EEG) seizure detection [51, 52] have been implemented. Advanced algorithms include complexity analysis procedures, such as approximate entropy (ApEn) calculation and ameliorate neurological disorders [53]. In our previous studies, we developed a multichannel open-loop stimulation system-on-chip (SoC) that is based on an open-source 8051 microcontroller for real-time data collection [54, 55]. Because no commercial embedded systems are available for neural phase synchrony stimulation and recording, we developed a closed-loop DSP platform using flexible FFT and a fully programmable stimulus control strategy, which considers parameters such as stimulation amplitude, frequency, and pulse width. This platform is flexible and adaptable to the electronic algorithm design, which is substantially advantageous in the first step of the investigation.

In the present study, an RISC processor [56] is the core of the closed-loop phase detection algorithm; it provides a flexible architecture and a uniform length instruction set that affords system implementation at various processing performance levels. At the system architecture level, a combination of programmable and digital circuits provides implementation feasibility to different algorithms. Hence, the major closed-loop phase detection algorithm and signal processing are set by the user, thus precisely controlling the stimulator. An analysis of the performance requirements in neural networks shows that the proposed microprocessor is adequate for signal processing. At the microarchitecture level, the processor performs feature extraction using diverse FFT resolutions for obtaining neural information. Additionally, a low-complexity algorithm for addition and multiplication was proposed for variable-FFT-length (16–1024 points) implementations that involve a tradeoff between memory bandwidth and run time. Using the proposed algorithm, continuous LFP signals were collected from freely moving PD rats. We focus on the phase interaction of the signal amplitude to achieve highly dynamic modulation of neural activity by using the phase of low-frequency rhythms. Hence, the proposed processor provides a platform for combined statistical testing in a closed-loop microstimulation, which enables onset pattern detection and provides a precise stimulus for adequate treatment of PD symptoms.

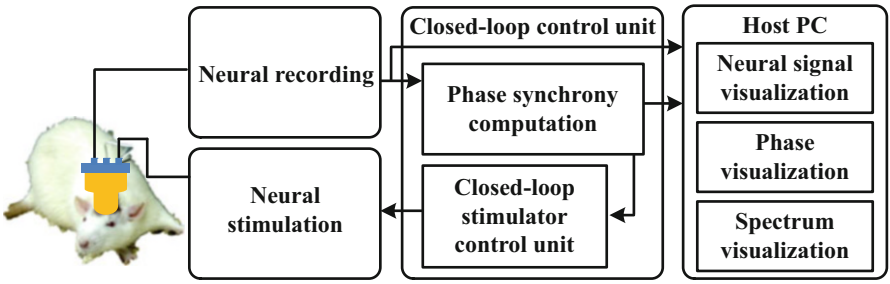

Fig. 10.5 Functional flow diagram of the closed-loop phase detection system. The digital signal processor is responsible for FFT, the control policy, and phase computation. In addition, the host PC can be used to rewrite the digital signal processor firmware, stimulation threshold, and to create a GUI for monitoring and storing data

10.5.2 System Architecture

The closed-loop phase detection system mainly consists of a recording analog front-end (AFE), a RISC processor, a stimulator, and a peripheral component interconnects. All external devices and algorithms are interconnected using a shared 32-bit data Wishbone bus, and the DSP, AFE, and analog-to-digital converter (ADC) interfaces can be connected in parallel with the crossbar switch. In addition, the host PC can rewrite processor firmware and monitor neural signal. The complete platform for closed-loop phase detection and the functional flow diagram is illustrated in Fig. 10.5.

10.5.2.1 Recording and Functional Electrical Stimulation

Adult (2-month-old) male Sprague Dawley rats weighing 250–350 g were used in this experiment. All animal handling, surgical, and behavior testing procedures were carried out in accordance with the guidelines on animal ethics. In each experiment, the rats were first anesthetized with chloral hydrate (400 g/kg) and urethane (0.5 g/kg). Microelectrodes were implanted into layer V of the M1 primary motor cortical region located using a stereotaxic apparatus with an average impedance of 50 kΩ at 130 Hz, after which the variable waveforms were recorded. Experimental experience has shown that a critical constraint in investigating neurophysiologic signals is that simultaneous recording of brain signals during DBS induces electrical artifacts several orders of amplitude larger than the brain waves. To overcome this constraint, investigators commonly adopt two distinct approaches. One approach involves recording the brain waves at the BG projection sites, where stimulation artifacts are less intense. The second approach, which we adopted in this study, involves avoiding stimulation artifacts by immediately recording brain waves after DBS. A 2-min M1 layer V time series was used for signal processing and statistical analysis on the host PC.

Data collection and the electrical stimulation architecture were based on our previous study. Deep brain signals were band-pass filtered between 0.1 and 700 Hz and amplified 3000-fold. A voltage-controlled stimulation (VCS) for a grounded load transmits the stimulation current to the tissues via the neural electrode. Through a programmable VCS interface implemented in the FPGA evaluation board, the user selects the RISC processor, sets the stimulation parameters, and stimulates the neurons.

10.5.2.2 Phase Analysis

Excessive synchronized oscillation in the beta frequency is one of the most common PD biomarker signals [14, 46] and a characteristic feature of the neural network activity in LFPs. However, the neuronal oscillations are quite inconsistent, and frequency spectra do not contain phase variant properties. On the basis of this knowledge, time-series fragmentation techniques are employed for analyzing intermittent synchronized oscillations to investigate the dynamic phase of synchronized signals, and the phase space of the brain signals is used to estimate the neural rhythms. The localized phase synchronizations are analyzed separately using frequency correlation. Each offline signal processing procedure is detailed for PC. All PC-based analyses were performed using MATLAB (The MathWorks, Natick, MA, USA). Before spectral analysis, raw data were band-pass filtered between 10 and 50 Hz to remove power-line noise and low-frequency oscillations. The time-varying power of neural changes in the motor state was estimated using short-time Fourier transform. Power changes were estimated using FFT with windows of 1024 samples, a Hanning window with a width of 0.5 s, and a 50 % overlap, until all signals were analyzed. In this time-varying spectral analysis, the high beta frequencies (20–35 Hz) of different relative power information were measured.

We detected localized phase synchronizations with respect to both time and frequency. Phase synchronizations were analyzed separately using a coherence technique. This technique involves obtaining the cross-spectrum of two signals by using the power spectral density. First, FFT is applied to both auto-power (P_{xx}) and cross-power spectra (P_{xy}).

$$P_{xx}(w) = E\left[|X(w)|^2\right], \tag{10.1}$$

$$P_{xy}(w) = E\left[X(w)Y(w)^*\right], \tag{10.2}$$

where $X(w)$ and $Y(w)$ are obtained using FFT of the time domain signals x(t) and y(t) (Fig. 10.6a). Next, phase relations are computed as follows:

$$\text{Phase}(w) = -\arctan\left(T_{xy}(w)\right) \tag{10.3}$$

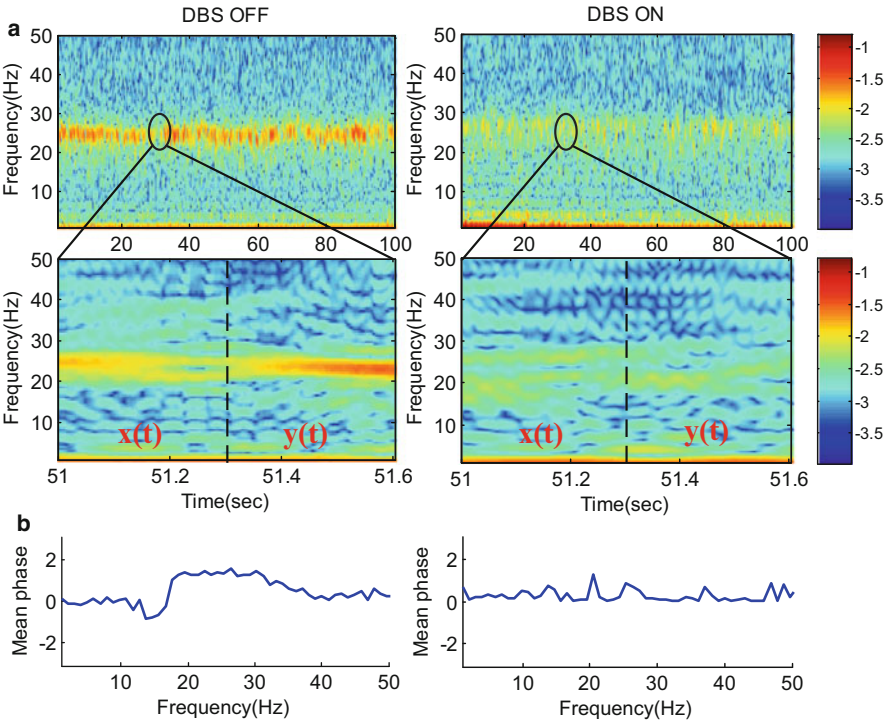

Fig. 10.6 LFP betas in the DBS ON and OFF states exhibit different characteristics. (**a**) Beta is observed in the 13–35 Hz range, where the power range is reduced and DBS ON and OFF is intermittently synchronous. The power ranges shown are plotted logarithmically. Time domain signals x(t) and y(t) are used to calculate the cross-spectrum and phase synchrony. (**b**) The mean phase (n = 37) is calculated for DBS ON and OFF, and the mean phase in DBS ON is more stable than that in DBS OFF

where $T_{xy}(w)$ is a transfer function based on the cross-spectrum of a signal pair; it is defined as

$$T_{xy}(w) = \frac{E\left[X(w)Y(w)^*\right]}{E\left[|X(w)|^2\right]} \tag{10.4}$$

All mean phases (n = 37) in the DBS ON and OFF states are presented in Fig. 10.6b. Phase relations refer to the periodicity labeling of the neural activity signals at a point between the coordinates (−3.141 to 3.141). On analyzing the beta frequency power time series, the phase series was found not to be a constant in the intermittent synchrony of power over time. The mean phase of DBS ON is more stable than that of DBS OFF. Therefore, adding phase time-series detection capability to a VCS system facilitates addressing neurobiological concerns.

10.5.2.3 Closed-Loop Stimulator Control Unit

As mentioned, neural phase dynamics can be calculated using the Fourier theory, and the phase equation of (10.1) enables the processor to activate the stimulator by using a precise threshold. The threshold condition of phase synchronization (PS) is defined as

$$\mathrm{PS} = \begin{cases} 1, & -\beta \times \pi \geq Phase(w) \geq \beta \times \pi \\ 0, & otherwise \end{cases} \tag{10.5}$$

where β is a constant determined using the statistical analysis presented in the subsequent paragraph. $\mathrm{PS} = 1$ activates the stimulator. In this study, precisely control of stimulator in short latency is a critical factor in maintaining the closed-loop system. An operational flowchart is depicted in Fig. 10.7.

A preliminary statistical analysis was performed to evaluate the start threshold β. Before determining the stimulation threshold, the continuous phase parameters were analyzed using paired t tests to evaluate the mean difference between stimulator ON and OFF states that maps β to an optimal stimulator start condition. Such analysis was performed on neural signals exhibiting PD symptoms. First, the phase characteristics of stimulator ON and OFF were independently tested for normality using the Shapiro–Wilk test. When the statistic is significant, the hypothesis that the distribution is normal is rejected. Second, another nonparametric statistical analysis, the paired t test, was performed to evaluate the differences in each pair. Significant p values were obtained in all cases.

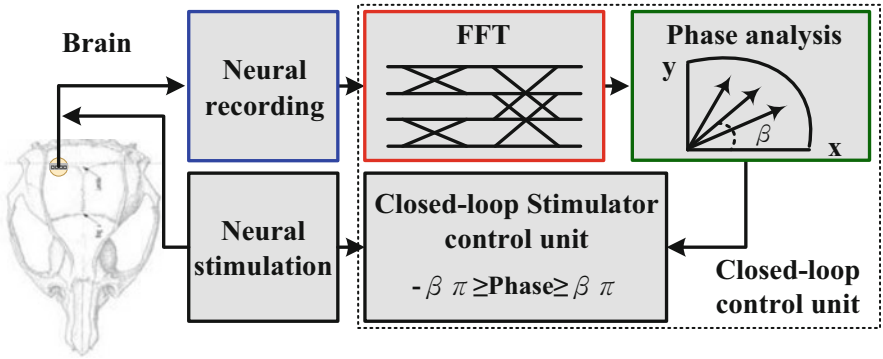

Fig. 10.7 System architecture of the closed-loop phase synchrony detection, consisting of a neural recording, a neural stimulation, and a closed-loop control unit. Closed-loop control unit covert the neural signal into phase domain and trigger stimulator when that phase synchrony exceeds a threshold

10.5.3 Real-Time Digital Processing Platform

Although our previous studies have successfully implemented 8051 microcontrollers in freely moving rats [54, 55], the architecture requires numerous instructions for a single operation. A high number of instructions can negatively affect the memory size, processing bandwidth, and real-time performance. Therefore, this study employed a 32-bit RISC processor, OpenRISC 1200 [56], for arithmetic operations, data storage, system control, and neural variant property evaluation. The 32-bit processor provides a computing speed of 2.1 DMIPS per MHz under the dhrystone benchmark and DSP MAC 32×32 operations per MHz. By contrast, the 8051 microcontroller in our previous studies computed at 1.67 DMIPS per MHz. In addition, virtual memory support, a five-stage pipeline, and basic capabilities are included in OpenRISC 1200. Processor efficiency and flexibility in specific tasks are crucial for precise and complex biomedical algorithms that sense neural activity.

The neural phase analysis of the system is classified into two components: First, the vector mode of the coordinate rotation digital computer (CORDIC) algorithm [57] is proposed, fulfilling the arctangent function, because it requires shift and add operations for each vector rotation. Because of the 16-bit fixed point computation in the processor, the word length of CORDIC computations must be considered for numerical accuracy. To achieve a 10-bit resolution of the fraction part [48], the word length should be at least $(n+\log_2 n+2)$, and $n+1$ rotations must be performed. Second, the variable point radix-2^4 FFT is proposed [58]. In the proposed RISC processor, this architecture achieves the lowest computing complexity for mathematical operations. In addition, the radix-2^4 algorithm provides a variable FFT length ranging from 16 to 1024 points. To increase FFT computation efficiency, the twiddle factor is precomputed, stored in an array in the processor memory, and accessed through table lookup.

Real-time signal processing for the closed-loop detection of localized phase synchronizations is implemented using a digital processor. The proposed algorithm and control policy can be verified on the implantable device firmware by using a wireless module. The firmware is segmented and updated independently and allows a series of instructions into the program memory from the boot ROM. The processor is programmed to deliver information as follows: (1) retrieve data from the SRAM and input it into the asynchronous FIFO; (2) set the stimulation parameters and the threshold for specific brain regions; and (3) start the N-point radix-2^4 FFT and CORDIC for phase computation.

After the phase property is calculated using the proposed algorithm, a hybrid approach is used where Fourier-based segmentation with phase synchrony is applied to maintain the neural activity reflected in the deep brain. Subsequently, the phase threshold condition β, which starts the stimulator, is trained statistically. When phase synchrony occurs, the processor generates a stimulation pulse. The initial programming setting generates a pulse width of 60 μs at a frequency of 125 Hz and amplitude of 5 V and supplies a constant current of 100 μA. These

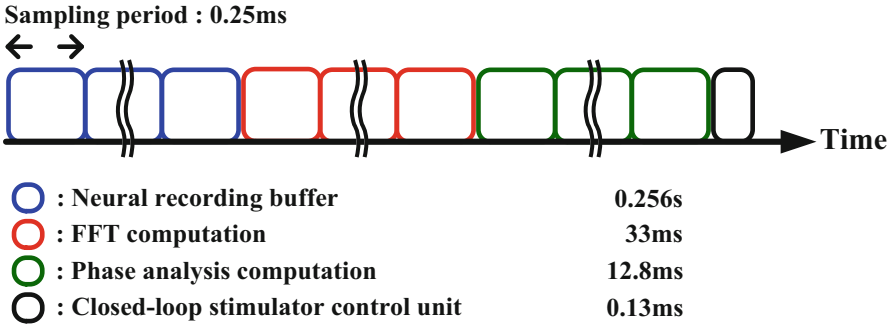

Fig. 10.8 Timing diagram of the phase detection firmware

parameters are effective in managing PD symptoms [59]; the user can flexibly modify the stimulation parameters by modifying the instruction set.

Detection latency is a critical factor in maintaining a real-time closed-loop system in which features of phase change are used to trigger stimulation. To evaluate the detection latency, an EEG dataset that generated output signals serving as AFE triggers was used. When one of the phase characteristics can trigger stimulation, it triggers the stimulator output and sets the identity of the detection unit, which is used in the feedback control scheme. The latency between a phase discriminator and a digital sample is then calculated using the same sample clock. A timing diagram of the experimental protocol is illustrated in Fig. 10.8. Closed-loop stimulation latencies were calculated using numerous individual subsystems, such as the digital sample, control policy, and phase detection algorithm. Using a 1024-point digital sample, the average run time for the asynchronous FIFO was 0.256 s. Furthermore, the phase detection latency calculated using the phase frequency and corresponding change in the Wishbone bus was determined for each firmware option. The difference in reaction latency for the RISC processor is largely attributable to the FFT and CORDIC; the mean latencies for the 1024-point FFT computation and CORDIC were 33 and 12.8 ms, respectively. Table 10.1 illustrates a comparison of the detection latency of the proposed system with those of recently published closed-loop systems. The shortest latency is reported in [53], where the sampling frequency is lower. Nevertheless, the 1024-point FFT and sampling frequency of our system is higher, and the neurological detect state is not the same. For the same neurological detect state, the shortest latency is in [60], where the test platform uses a software and hardware coworker but does not consider the sampling time.

10.5.4 Implementation Results

An ALTERA DE2-115 FPGA evaluation board, capable of reloading instructions and implanted with dedicated RISC processors, was used to verify the functionality and basic control policy. The processor instructions were stored in a 2 MB SRAM; a

Table 10.1 Comparison of the proposed system with recent systems

	[60]	[53]	[51]	[23]	This work
DSP operation	Empirically derived linear threshold on the amplitude	Programmable, 64-point FFT (radix-4), and on-line seizure detection	256-point FFT (radix-2)	LFP amplitude threshold for triggering stimulation	**Flexible N-point FFT (N = 16 through 1024) (Radix-2^4)**
Processor	PC	OR1200	Cortex-M3	Embedded processor (Spike 2 software)	**OR1200**
Latency	0.600 s	0.500–0.800 s	>0.500 s	>0.030–0.040 s[a] + x	**0.302 s (N = 1024) 0.550 s (N = 256, 5 MHz) 0.114 s (N = 64, 13.6 MHz)**
Sampling frequency	422 Hz	200 Hz	256 Hz	1 kHz	**4 kHz**
Operating frequency	N/A	13.6 MHz	7 kHz (0.5 V) 5 MHz (1 V)	N/A	**25 MHz**
Neurological state	LFP, EMG, ECoG	Epilepsy	Epilepsy	LFPs	**LFPs, EMG, sEEG**

[a]*x* without consider 0.400 s moving average filter, digital sample, and software and hardware interface delay time
N/A Not Available

waveform generator was used to store the EEG dataset and regenerate the brain signal for the digital processors. The EEG datasets were collected from our previous study. Figure 10.9 showed the top view of the recording system and a rat implanted with the neuron-probes. In addition, the EEG dataset was used to demonstrate the functionality of the system: data collection, phase characteristic identification, and compatibility with the closed-loop algorithm and the evaluation board.

After the system is initiated, the user can rewrite the firmware codes and start the RISC processors, which can access digital samples directly from the ADCs (waveform generators) and continuously perform phase detection. To facilitate validating the dynamic phase and the stimulator control policy states, the experimental results are streamed in real time to the host PC through a wireless module so that the user can monitor the algorithm operation.

A specific example is the closed-loop DBS for PD, which entails (1) capturing neural signals by controlling the ADC sampling clock; (2) statistically determining the stimulation threshold; and (3) evaluating the phase synchronization through DSP.

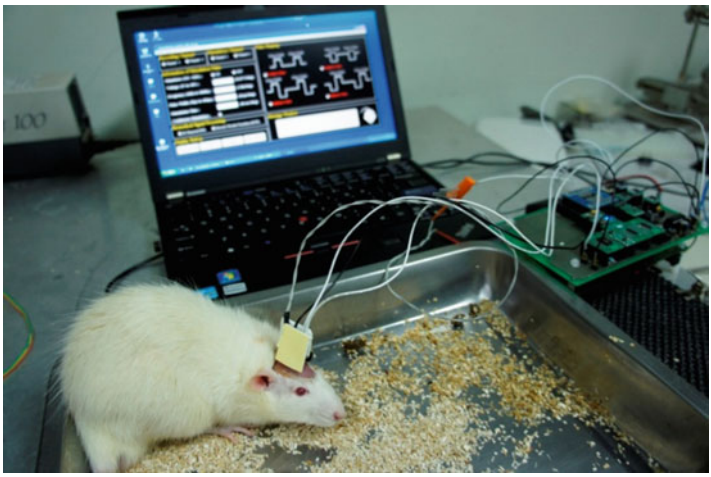

Fig. 10.9 Data collection and electrical stimulation

10.5.4.1 Data Collection

The digital samples are loaded into a waveform generator and output to a 12-bit ADC. The sampling frequency for the neural signal is 4 kHz, and system operation at 25 MHz is adequate for real-time signal processing. Subsequently, the processor has a buffer for retrieving 1024 digital samples through a parallel interface. FFT, CORDIC, and phase are computed for the next 1024 digital samples and phase synchronizations are subsequently detected. The experiment was completed in approximately 2 min. After using the timing diagram to design the firmware, the default instructions are written to the processor; handshakes with the host PC ensure that the data are passed correctly, subsequently; the user sets the stimulation parameters and controls the ADC.

10.5.4.2 Statistical Results

Statistical analyses were performed using the R 3.1.1 software (R Foundation for Statistical Computing, Vienna, Austria). A two-sided p value less than 0.05 was considered statistically significant. Data were expressed as the mean $\pm$ standard deviation. The continuous data of DBS ON and OFF were assessed using the paired t test. Forty data records for DBS ON and OFF, each measured 40 times, were included. Three data signals were excluded because of poor data recording and incomplete recording of brain signals.

All data ($n = 37$) are presented in Table 10.2. The mean phases of DBS ON and OFF show statistically significant (1.084 ± 0.748 vs. 1.600 ± 0.864; $p = 0.002$) that using the paired t test. Normality for DBS ON and OFF was statistically significant

Table 10.2 Effect of electrical stimulation on phase response

	ON	OFF	
Phase	1.084 ± 0.748	1.600 ± 0.864	$p = 0.002$
Shapiro–Wilk test: DBS ON: $p = 0.180$, DBS OFF: $p = 0.113$			

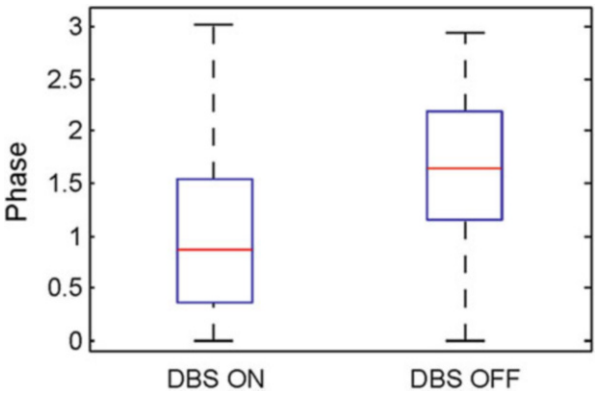

Fig. 10.10 Box–Whisker plot of phase suppression of the beta band. Suppression of phase synchrony of LFPs occurs between 20 and 35 Hz in the DBS ON and OFF states

($p = 0.180$, $p = 0.113$). Figure 10.10 showed the Box–Whisker plot of phase suppression. According to this statistical result, the stimulation threshold based on DBS OFF was sets 1.6°.

10.5.4.3 Phase Synchronization Detection in the EEG Dataset

For detecting phase suppression, the transfer function that measures the signal of synchronous change over short-time intervals is calculated. Every 0.256 s, a 1024-point FFT is performed for the input data with a 50 % overlap in time, followed by the execution of the CORDIC algorithm. Phase synchronization is determined using two 1024-sample cycles along with DSP; phase response detection takes approximately 0.302 s.

Neural recording of M1 layer V stimulation artifacts during electrical stimulation at 125 Hz and pulse width of 60 μs is presented in Fig. 10.11a. To evaluate the effect of electrical stimulation on phase detection, neural signals after DBS (Fig. 10.11b) are used as a dataset for DSP. Figure 10.11c, d shows a 0.302 s segment of the 1024-point FFT and phase irregular stimulation pattern; the upper panels depict power and phase detection events for triggering stimulation. These signals were recorded to determine whether the LFP power spectra and phase were consistent across each segment of the time series despite interventions such as DBS ON or OFF states. In each segment, the signal that differed indicates that the power and phase in the beta range triggered stimulation.

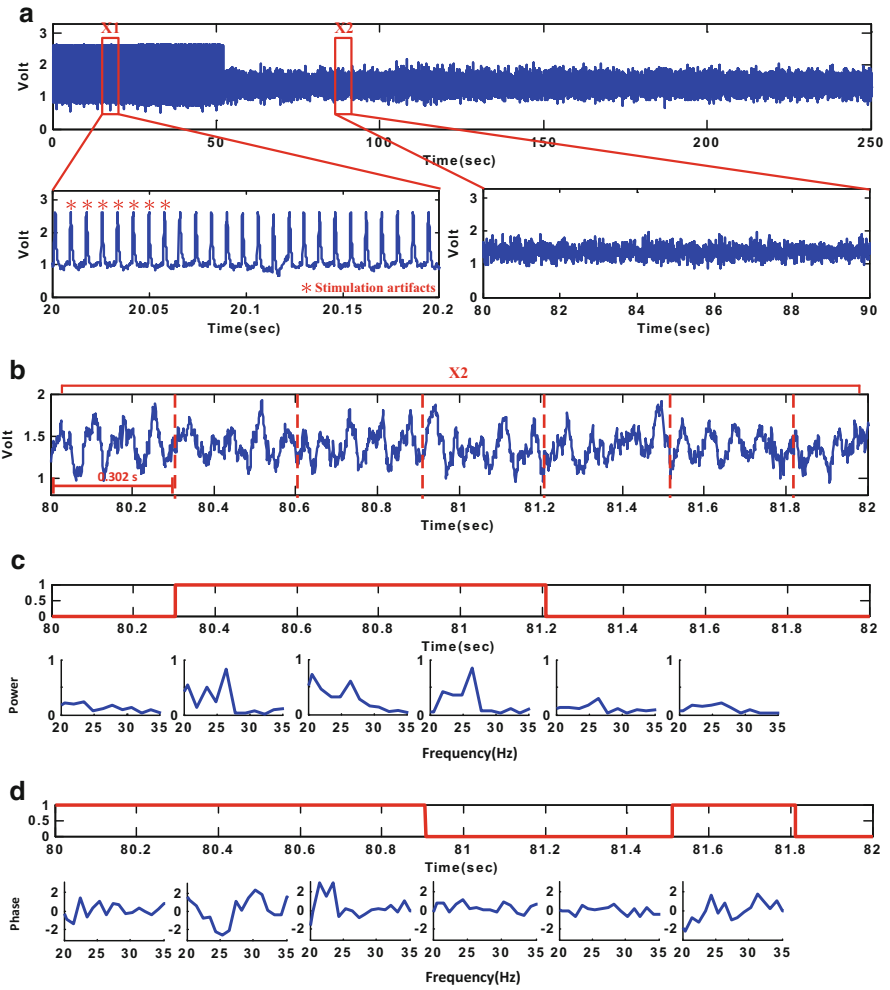

Fig. 10.11 Two-second series analysis in detecting the fine temporal structure of intermittent power spectrum and phase synchrony. (**a**) An example of a 250 s LFP neural signal S1 before showing stimulation artifacts and S2 after applying the stimulus paradigm. (**b**) Neural recording for 2 s after electrical stimulation. (**c**, **d**) 0.302 s trace of the stimulation pattern; 1024-point FFT and phase irregular stimulation pattern

10.5.4.4 Comparison with Other Studies

The foundation of the closed-loop system is related to choose the neural data as a biomarker. All techniques have its advantage, depending on the different algorithm and practical system constraints. Table 10.3 lists the results of the phase detection algorithm compared with monitor power spectrum when that power exceeds a stimulation threshold in the specific frequency band [38] and LFPs oscillations

Table 10.3 Summary of power spectrum, LFP AMPLITUDE, and phase synchrony detections

	[38]	[23]	This work
Stimulation times	371 ± 14	358 ± 31	302 ± 21

was used to control triggered stimulator via a defined threshold [23]. In addition, the EEG dataset ($n = 37$) was used to demonstrate the functionality of the closed-loop system and the total duration for all experiments was nearly 2 min.

To evaluate the closed-loop effect of electrical stimulation on power spectrum, LFPs oscillations and phase synchrony detection, the numbers of triggered stimulator are used as an indicator in this experiment. In an open-loop system, the total detection number is 397, without considering the stimulation threshold. And then closed-loop spectrum detection and LFPs oscillation detection need 371 and 358 times stimulation. Our proposed method requires 302 times stimulation. Hence, the selection of features for detection has important implications for power consumption.

As a result, the spectrum, LFPs oscillations, and phase synchrony detection numbers represent distinct phenomena (Fig. 10.12) and Fig. 10.12d showing that our proposed method in the beta frequency band has a lower percentage of triggered stimulator over time. These three methods were individually significant in the EEG dataset (LFPs amplitude, phase synchrony, and power spectrum; $p < 0.001$) and exhibit a positive relationship over time.

In this study, a real-time closed-loop neurostimulation system should be able to provide localized phase detection and precise control of electrical stimulation for in-vivo experiments; accordingly, such in-vivo experiments have to be considered for the next step of experimentation.

10.6 Conclusions

With the development of bioelectronics, DSP, and effective feedback loops for maintaining neurotransmitters, the closed-loop DBS system is playing a growing role in the treatment of certain medical conditions. Precise control of electrical stimulation requires an advanced signal processing algorithm that maintains therapeutic efficacy at optimal levels. Through detailed analysis of typical closed-loop DBS systems, this chapter has presented an overview of neural recording systems, stimulation systems, and digital integrated circuits. The specifications of each function have been presented.

A real-time closed-loop neurostimulation system based on a neural phase synchrony detection design has also been discussed. We developed a closed-loop digital signal processor platform using the radix-2^4 algorithm, providing a variable FFT length ranging from 16 to 1024 points with a short latency response (0.302 s) and offering fully programmable stimulation. This study focused on the use of transfer-function-based LFP processing for calculating phase synchrony, which

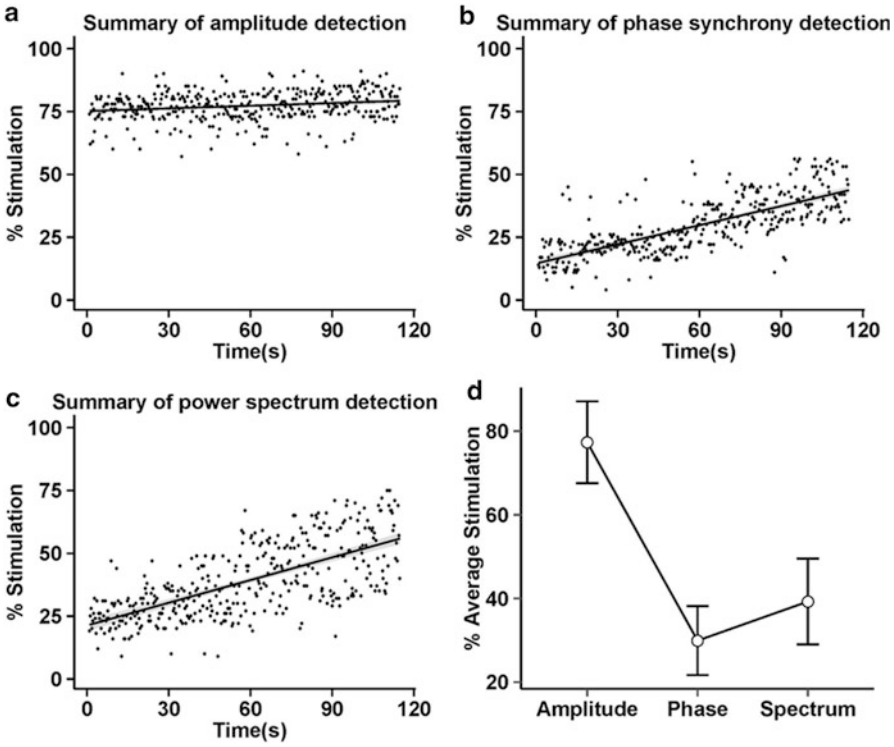

Fig. 10.12 The percentage of triggered stimulator over time (% per 0.302 s block). The solid line is result of linear regression. (**a**) The percentage of LFPs amplitude triggered stimulator. Multiple R-squared is 0.537, $p < 0.001$. (**b**) The percentage of phase synchrony triggered stimulator. Multiple R-squared is 0.482, $p < 0.001$. (**c**) The percentage of phase synchrony triggered stimulator. Multiple R-squared is 0.512, $p < 0.001$. (**d**) Mean and standard error of the percentage of triggered stimulator with different stimulation conditions

was then used to trigger the neural stimulator. A preliminary statistical analysis provided additional evidence that the feedback threshold parameters can be optimized and directly transferred to fit the threshold conditions. Advanced statistical methods can then be used to address neurobiological problems. Finally, the proposed method can be extended to other biomedical signal applications such as electromyography and surface EEG. Commercial platforms can be employed to conduct short-term experiments and functional verification, whereas ICs are more practical for specific and long-term applications.

References

1. Harrison RR (2007) A versatile integrated circuit for the acquisition of biopotentials. Custom integrated circuits conference, p 115–122
2. Kultas-Ilinsky K, Ilinsky IA (2001) Basal Ganglia and Thalamus in health and movement disorders. Springer, New York
3. Lozano AM, Gildenberg PL, Taske RR (2009) Textbook of stereotactic and functional neurosurgery. Springer, Berlin and Heidelberg
4. Perlin GE, Sodagar AM, Wise KD (2006) Neural recording front-end designs for fully implantable neuroscience applications and neural prosthetic microsystems. Engineering in Medicine and Biology Society, p 2982–2985
5. Lopez-Azcarate J, Tainta M, Rodriguez-Oroz MC, Valencia M, Gonzalez R, Guridi J et al (2010) Coupling between beta and high-frequency activity in the human subthalamic nucleus may be a pathophysiological mechanism in Parkinson's disease. J Neurosci 30:6667–6677
6. Schuurman PR, Bosch DA, Bossuyt PMM, Bonsel GJ, van Someren EJW, de Bie RMA et al (2000) A comparison of continuous thalamic stimulation and thalamotomy for suppression of severe tremor. N Engl J Med 342:461–468
7. Fisher R, Salanova V, Witt T, Worth R, Henry T, Gross R et al (2010) Electrical stimulation of the anterior nucleus of thalamus for treatment of refractory epilepsy. Epilepsia 51:899–908
8. Halpern CH, Samadani U, Litt B, Jaggi JL, Baltuch GH (2008) Deep brain stimulation for epilepsy. Neurotherapeutics 5:59–67
9. Mayberg HS, Lozano AM, Voon V, McNeely HE, Seminowicz D, Hamani C et al (2005) Deep brain stimulation for treatment-resistant depression. Neuron 45:651–660
10. Schoenen J, Di Clemente L, Vandenheede M, Fumal A, De Pasqua V, Mouchamps M et al (2005) Hypothalamic stimulation in chronic cluster headache: a pilot study of efficacy and mode of action. Brain 128:940–947
11. Leone M, Franzini A, Bussone G (2001) Stereotactic stimulation of posterior hypothalamic gray matter in a patient with intractable cluster headache. N Engl J Med 345:1428–1429
12. Loukas C, Brown P (2012) A PC-based system for predicting movement from deep brain signals in Parkinson's disease. Comput Methods Programs Biomed 107:36–44
13. de Haas R, Struikmans R, van der Plasse G, van Kerkhof L, Brakkee JH, Kas MJ et al (2012) Wireless implantable micro-stimulation device for high frequency bilateral deep brain stimulation in freely moving mice. J Neurosci Methods 209:113–119
14. Meissner W, Leblois A, Hansel D, Bioulac B, Gross CE, Benazzouz A et al (2005) Subthalamic high frequency stimulation resets subthalamic firing and reduces abnormal oscillations. Brain 128:2372–2382
15. McCracken CB, Kiss ZHT (2014) Time and frequency-dependent modulation of local field potential synchronization by deep brain stimulation. PLoS One 9, http://journals.plos.org/plosone/article?id=10.1371/journal.pone.0102576
16. Rosin B, Slovik M, Mitelman R, Rivlin-Etzion M, Haber SN, Israel Z et al (2011) Closed-loop deep brain stimulation is superior in ameliorating Parkinsonism. Neuron 72:370–384
17. Santaniello S, Fiengo G, Glielmo L, Grill WM (2011) Closed-loop control of deep brain stimulation: a simulation study. IEEE Trans Neural Syst Rehabil Eng 19:15–24
18. Jochum T, Denison T, Wolf P (2009) Integrated circuit amplifiers for multi-electrode intracortical recording. J Neural Eng 6, http://www.ncbi.nlm.nih.gov/pubmed/19139560
19. Gesteland RC, Howland B, Lettvin JY, Pitts WH (1959) Comments on microelectrodes. Proc IRE 47:1856–1862
20. Priori A, Foffani G, Rossi L (2005) Apparatus for treating neurological disorders by means of adaptive electro-stimulation retroacted by biopotentials. European Patent Office
21. Rouse AG, Stanslaski SR, Cong P, Jensen RM, Afshar P, Ullestad D, et al (2011) A chronic generalized bi-directional brain-machine interface. J Neural Eng 8, http://www.ncbi.nlm.nih.gov/pubmed/21543839

22. Nowak K, Mix E, Gimsa J, Strauss U, Sriperumbudur KK, Benecke R, et al (2011) Optimizing a rodent model of Parkinson's disease for exploring the effects and mechanisms of deep brain stimulation. Park Dis 2011, http://www.ncbi.nlm.nih.gov/pubmed/21603182
23. Little S, Pogosyan A, Neal S, Zavala B, Zrinzo L, Hariz M et al (2013) Adaptive deep brain stimulation in advanced Parkinson disease. Ann Neurol 74:449–457
24. Afshar P, Khambhati A, Stanslaski S, Carlson D, Jensen R, Linde D et al (2012) A translational platform for prototyping closed-loop neuromodulation systems. Front Neural Circ 6:117
25. Lobel DA, Lee KH (2014) Brain machine interface and limb reanimation technologies: restoring function after spinal cord injury through development of a bypass system. Mayo Clin Proc 89:708–714
26. Avestruz AT, Santa W, Carlson D, Jensen R, Stanslaski S, Helfenstine A et al (2008) A 5 uW/channel spectral analysis IC for chronic bidirectional brain-machine interfaces. IEEE J Solid State Circuits 43:3006–3024
27. Nunez P (1981) Electric fields of the brain: the neurophysics of EEG. Oxford University Press, New York
28. Zhang K, Ginzburg I, McNaughton BL, Sejnowski TJ (1998) Interpreting neuronal population activity by reconstruction: unified framework with application to hippocampal place cells. J Neurophysiol 79:1017–1044
29. Burke MJ, Gleeson DT (2000) A micropower dry-electrode ECG preamplifier. IEEE Trans Biomed Eng 47:155–162
30. Spinelli EM, Martinez N, Mayosky MA, Pallas-Areny R (2004) A novel fully differential biopotential amplifier with DC suppression. IEEE Trans Biomed Eng 51:1444–1448
31. Oppenheim AV, Schafer RW (2009) Discrete-time signal processing. Prentice Hall
32. Proakis JG, Manolakis DG (1996) Digital signal processing: principles, algorithms, and applications, 3rd ed. Prentice-Hall
33. Psatta DM (1983) Control of chronic experimental focal epilepsy by feedback caudatum stimulations. Epilepsia 24:444–454
34. Hamani C, Diwan M, Isabella S, Lozano AM, Nobrega JN (2010) Effects of different stimulation parameters on the antidepressant-like response of medial prefrontal cortex deep brain stimulation in rats. J Psychiatr Res 44:683–687
35. McCracken CB, Grace AA (2009) Nucleus accumbens deep brain stimulation produces region-specific alterations in local field potential oscillations and evoked responses in vivo. J Neurosci 29:5354–5363
36. McIntyre CC, Chaturvedi A, Shamir RR, Lempka SF (2015) Engineering the next generation of clinical deep brain stimulation technology. Brain Stimul 8:21–26
37. Suresh DC, Agrawal B, Yang J, Najjar W (2005) A tunable bus encoder for off-chip data buses. Presented at the proceedings of the 2005 international symposium on Low power electronics and design
38. Priori A, Foffani G, Rossi L, Marceglia S (2013) Adaptive deep brain stimulation (aDBS) controlled by local field potential oscillations. Exp Neurol 245:77–86
39. Romrell J, Fernandez HH, Okun MS (2003) Rationale for current therapies in Parkinson's disease. Expert Opin Pharmacother 4:1747–1761
40. Deep-brain stimulation of the subthalamic nucleus or the pars interna of the globus pallidus in Parkinson's disease (2001). N Engl J Med 345:956–963, http://www.ncbi.nlm.nih.gov/pubmed/11575287
41. Kleiner-Fisman G, Fisman DN, Sime E, Saint-Cyr JA, Lozano AM, Lang AE (2003) Long-term follow up of bilateral deep brain stimulation of the subthalamic nucleus in patients with advanced Parkinson disease. J Neurosurg 99:489–495
42. Fishman PS (2008) Paradoxical aspects of Parkinsonian tremor. Mov Disord 23:168–173
43. Dostrovsky JO, Lozano AM (2002) Mechanisms of deep brain stimulation. Mov Disord 17 (Suppl 3):S63–S68
44. Bronte-Stewart H, Taira T, Valldeoriola F, Merello M, Marks WJ Jr, Albanese A et al (2011) Inclusion and exclusion criteria for DBS in dystonia. Mov Disord 26(Suppl 1):S5–S16

45. Eusebio A, Thevathasan W, Gaynor LD, Pogosyan A, Bye E, Foltynie T et al (2011) Deep brain stimulation can suppress pathological synchronisation in Parkinsonian patients. J Neurol Neurosurg Psychiatry 82:569–573
46. McCracken CB, Kiss ZH (2014) Time and frequency-dependent modulation of local field potential synchronization by deep brain stimulation. PLoS One 9, http://www.ncbi.nlm.nih.gov/pubmed/16123144
47. Park C, Worth RM, Rubchinsky LL (2010) Fine temporal structure of beta oscillations synchronization in subthalamic nucleus in Parkinson's disease. J Neurophysiol 103:2707–2716
48. Silberstein P, Pogosyan A, Kuhn AA, Hotton G, Tisch S, Kupsch A et al (2005) Cortico-cortical coupling in Parkinson's disease and its modulation by therapy. Brain 128:1277–1291
49. Venkatraman S, Elkabany K, Long JD, Yao Y, Carmena JM (2009) A system for neural recording and closed-loop intracortical microstimulation in awake rodents. IEEE Trans Biomed Eng 56:15–22
50. Angotzi GN, Boi F, Zordan S, Bonfanti A, Vato A (2014) A programmable closed-loop recording and stimulating wireless system for behaving small laboratory animals. Sci Rep 4: 15–22
51. Sridhara SR, DiRenzo M, Lingam S, Seok-Jun L, Blazquez R, Maxey J et al (2011) Microwatt embedded processor platform for medical system-on-chip applications. IEEE J Solid State Circuits 46:721–730
52. Verma N, Shoeb A, Bohorquez J, Dawson J, Guttag J, Chandrakasan AP (2010) A micro-power EEG acquisition SoC with integrated feature extraction processor for a chronic seizure detection system. IEEE J Solid State Circuits 45:804–816
53. Chen T-J, Chiueh H, Liang S-F, Chang S-T, Jeng C, Hsu Y-C (2011) The implementation of a low-power biomedical signal processor for real-time epileptic seizure detection on absence animal models. IEEE J Emerging Sel Top Circ Syst 1:613–621
54. Lin YP, Yeh CY, Huang PY, Wang ZY, Cheng HH, Li YT, et al (2015) A battery-less, implantable neuro-electronic interface for studying the mechanisms of deep brain stimulation in rat models. IEEE Trans Biomed Circ Syst, http://ieeexplore.ieee.org/xpl/login.jsp?tp=&arnumber=6081950&url=http%3A%2F%2Fieeexplore.ieee.org%2Fxpls%2Fabs_all.jsp%3Farnumber%3D6081950
55. Chun-Yi Y, Hung-Chih C, Hsi-Pin M (2013) An information hub for implantable wireless brain machine interface. 2013 international symposium on VLSI design, automation, and test (VLSI-DAT), p 1–4
56. Damjan Lampret JB, OpenRISC 1200 IP core specification (preliminary draft) [Online]. http://opencores.org/websvn,filedetails?repname=openrisc&path=%2Fopenrisc%2Ftrunk%2For1200%2Fdoc%2Fopenrisc1200_spec.pdf&rev=645
57. Andraka R (1998) A survey of CORDIC algorithms for FPGA based computers. Presented at the proceedings of the 1998 ACM/SIGDA sixth international symposium on field programmable gate arrays, Monterey, CA
58. Ayinala M, Parhi KK (2013) FFT architectures for real-valued signals based on radix-2(3) and radix-2(4) algorithms. IEEE Trans Circ Syst I-Reg Papers 60:2422–2430
59. Wojtecki L, Vesper J, Schnitzler A (2011) Interleaving programming of subthalamic deep brain stimulation to reduce side effects with good motor outcome in a patient with Parkinson's disease. Parkinsonism Relat Disord 17:293–294
60. Isaacson B, Dani S, Desai SA, Denison T, Afshar P (2013) A rapid algorithm prototyping tool for bi-directional neural interfaces. 2013 6th international IEEE/EMBS conference on neural engineering (NER), p 633–636